Multibody Syst Dyn (2012) 27:153–171
DOI 10.1007/s11044-011-9269-4

# First order sensitivity analysis of flexible multibody systems using absolute nodal coordinate formulation

**Ting Pi · Yunqing Zhang · Liping Chen**

Received: 8 August 2010 / Accepted: 1 June 2011 / Published online: 1 July 2011


**Abstract** Design sensitivity analysis of flexible multibody systems is important in optimizing the performance of mechanical systems. The choice of coordinates to describe the motion of multibody systems has a great influence on the efficiency and accuracy of both the dynamic and sensitivity analysis. In the flexible multibody system dynamics, both the floating frame of reference formulation (FFRF) and absolute nodal coordinate formulation (ANCF) are frequently utilized to describe flexibility, however, only the former has been used in design sensitivity analysis. In this article, ANCF, which has been recently developed and focuses on modeling of beams and plates in large deformation problems, is extended into design sensitivity analysis of flexible multibody systems. The Motion equations of a constrained flexible multibody system are expressed as a set of index-3 differential algebraic equations (DAEs), in which the element elastic forces are defined using nonlinear strain-displacement relations. Both the direct differentiation method and adjoint variable method are performed to do sensitivity analysis and the related dynamic and sensitivity equations are integrated with HHT-I3 algorithm. In this paper, a new method to deduce system sensitivity equations is proposed. With this approach, the system sensitivity equations are constructed by assembling the element sensitivity equations with the help of invariant matrices, which results in the advantage that the complex symbolic differentiation of the dynamic equations is avoided when the flexible multibody system model is changed. Besides that, the dynamic and sensitivity equations formed with the proposed method can be efficiently integrated using HHT-I3 method, which makes the efficiency of the direct differentiation method comparable to that of the adjoint variable method when the number of design variables is not extremely large. All these improvements greatly enhance the application value of the direct

T. Pi · Y. Zhang (✉) · L. Chen
Center for Computer-Aided Design, School of Mechanical Science & Engineering, Huazhong University of Science & Technology, Wuhan, Hubei 430074, China
e-mail: zhangyq@hust.edu.cn

T. Pi
e-mail: piting007@gmail.com

L. Chen
e-mail: chenlp@hustcad.com

differentiation method in the engineering optimization of the ANCF-based flexible multibody systems.

**Keywords** ANCF · Direct differentiation method · Adjoint variable method · HHT-I3 · Invariant matrices

## 1 Introduction

Optimizing the performance of mechanical systems is one of the most important objectives and applications of multibody system dynamics. Gradient based optimization methods may greatly improve the efficiency and convergence rate of the optimization process by providing sensitivity information. In this sense, sensitivity analysis plays a key role in bridging the gaps between optimization and dynamic analysis.

Design sensitivity analysis has been developed for almost 40 years and four different methods have been developed: the finite difference method, direct differentiation method, adjoint variable method, and automatic differentiation method. Among them, the finite difference method [15] is the simplest, which uses perturbed parameters to calculate sensitivities of the objective function with respect to design variables. However, this method is very time consuming and results in the difficulty in choosing the perturbation [15]. A large step size may lead to unacceptable truncation errors while a small one may result in undesirable round off errors. The third drawback is the poor numerical performance which is derived from the need of additional analysis for the perturbation of each additional design variable [17].

Different from finite difference method, the direct differentiation method and adjoint variable method belong to analytical methods. The direct differentiation method [10, 11, 18–21, 26, 28, 31, 33, 34, 39] is easy to understand, which obtains the sensitivity equations by differentiating the dynamic equations with respect to design variables in accordance with the chain rule of differentiation. The sensitivity equations are then integrated simultaneously with the dynamic equations to obtain the derivatives of state variables, and Lagrange multipliers in the case of DAEs, with respect to design variables. After that, sensitivities of the objective or performance function with respect to design variables can be easily evaluated. The attractive advantage of direct differentiation is the effective control of time integration errors when implicit numerical methods are used. However, it needs a large number of sensitivity equations to be derived analytically and integrated if there are a large number of design variables and state variables, which is cumbersome and error-prone. The situation is even worse when this method is applied to the sensitivity analysis of flexible multibody systems. If the flexible part is modeled with the finite element method and the number or the type of finite elements is modified frequently, it is heavy work to deduce these equations.

The adjoint variable method [4, 5, 9, 11, 20, 24, 25] introduces a set of adjoint variables to circumvent explicit calculation of state sensitivities. Firstly, dynamic equations are calculated forwards to obtain the state variables and Lagrange multipliers. Secondly, the adjoint equations are integrated backward to obtain the adjoint variables. Finally, the derivatives of objective functions with respect to design variables are evaluated. The main advantage of this method compared with direct differentiation method is that the number of DAE systems to be integrated is greatly reduced if there are a large number of design variables, which saves a lot of computation time. However, there are mainly two drawbacks. First, the construction of adjoint equations is complicated. Second, a large number of input and output operations are required and the error control of the backward integration is difficult.

Automatic differentiation method is an approach for efficiently calculating the derivatives of functions. Adifor [7, 8, 13] is a representation of this method, which is able to generate the partial derivatives of the source code with respect to the user-defined design variables. The efficiency of automatic differentiation method is not clear compared with the three methods discussed above [16]. Valuable suggestions to obtain reliable results with this method are proposed in [31].

Research on sensitivity analysis of multibody systems mainly focuses on rigid multibody systems and literature on sensitivity analysis of flexible multibody systems is sparse [6, 11]. In these papers, the flexible multibody systems are formulated using FFRF, which is the most widely used way to describe flexibility. FFRF uses two sets of coordinates to describe the configuration of the deformable bodies; one set describes the position and orientation of a body fixed coordinate system, and the other describes the deformation of the body with respect to its body fixed coordinate system. As a consequence, the stiffness matrix used to obtain elastic forces remains the same. However, the mass matrix, centrifugal, and Coriolis inertia forces and even generalized gravity forces appear highly nonlinear in this approach. Moreover, the small deformation assumption limits the use of FFRF in large deformation problems.

Three other description methods applied to simulating flexible multibody systems are the incremental finite element approach, large rotation vector formulation and ANCF [36]. The incremental finite element approach introduces infinitesimal rotation angles as nodal variables to overcome the limitation of FFRF. However, this approach cannot exactly describe the rigid-body motion, which is an important issue in flexible multibody dynamics. The large rotation vector formulation replaces the infinitesimal rotation angles of incremental finite element approach with finite ones so that the rigid-body displacement can be exactly described. However, this method has not been widely accepted due to the redundancy of representing the large rotation of the cross section which may lead to singularity problems and unrealistic shear forces.

ANCF [35, 37, 40] introduces absolute displacements and global slopes as nodal coordinates with respect to the global reference frame, which is significantly different from the other three formulations mentioned above. This difference prevents the terms of motion equations from being highly nonlinear because the mass matrix and generalized force remain constant and centrifugal and Coriolis inertia forces equal zero in this situation. The only nonlinear term is the elastic forces vector. However, recent research [14] has developed an efficient procedure for evaluating the elastic forces, the elastic energy and the Jacobian matrix of the elastic forces. ANCF is able to achieve the exact modeling of the rigid body modes and be used to solve large deformation problems while FFRF is just effective in the range of small deformation situation.

This paper extends ANCF to the first order sensitivity analysis of flexible multibody systems using both direct differentiation method and adjoint variable method. As far as the authors' knowledge, this topic has not been discussed before. In Sect. 2, the dynamic analysis of the ANCF-based flexible multibody systems and the corresponding computational strategy are presented. Section 3 describes the first order sensitivity analysis of the flexible multibody systems, including both the direct differentiation method and adjoint variable method. A new method to deduce sensitivity equations is proposed in this section. Two numerical experiments are performed to verify the feasibility and efficiency of the proposed method in Sect. 4. Section 5 gives a conclusion at last.

## 2 Dynamics of flexible multibody systems based on ANCF

This section presents the formulation of system dynamic equations and the corresponding computation strategy at first. Then the terms of system equations based on ANCF are described. Jacobian matrix of the elastic forces vector, which is required by the computation strategy, is presented at last.

### 2.1 Equations of motion and computational strategy

Different kinds of system equations for constrained multibody systems have been proposed over the years [1, 23]. This paper adopts the frequently used DAE system of index-3 with holonomic constraints which is usually written as

$$\begin{aligned} \boldsymbol{M}(\boldsymbol{q},\boldsymbol{b})\ddot{\boldsymbol{q}} + \boldsymbol{\Phi}_{\boldsymbol{q}}^T\boldsymbol{\lambda} &= \boldsymbol{Q}_s(\boldsymbol{q},\boldsymbol{b},t) + \boldsymbol{Q}_e(\dot{\boldsymbol{q}},\boldsymbol{q},\boldsymbol{b},t), \\ \boldsymbol{\Phi}(\boldsymbol{q},\boldsymbol{b}) &= \boldsymbol{0}, \end{aligned} \tag{1}$$

where $\boldsymbol{\Phi}_{\boldsymbol{q}}$ is the Jacobian matrix of the constraints $\boldsymbol{\Phi}$, $\boldsymbol{Q}_e$ and $\boldsymbol{Q}_s$ are the vectors of generalized external and elastic forces, respectively, $\boldsymbol{\lambda}$ is the vector of Lagrange multipliers, $\boldsymbol{q}$, $\dot{\boldsymbol{q}}$ and $\ddot{\boldsymbol{q}}$ are the vectors of general displacement, velocity, and acceleration coordinates, respectively, $t$ is the time variable and $\boldsymbol{b}$ is the vector of design variables. In this paper, an assumption is made that the most widely used geometry and material parameters are chosen as design variables.

To solve (1), the newly proposed HHT-I3 method [29] is employed. In the HHT-I3 algorithm, the position and velocity variables of step $n+1$ are defined as

$$\boldsymbol{q}_{n+1} = \boldsymbol{q}_n + h\dot{\boldsymbol{q}}_n + \frac{h^2}{2}\big[(1-2\beta)\boldsymbol{a}_n + 2\beta\boldsymbol{a}_{n+1}\big], \tag{2}$$

$$\dot{\boldsymbol{q}}_{n+1} = \dot{\boldsymbol{q}}_n + h\big[(1-\gamma)\boldsymbol{a}_n + \gamma\boldsymbol{a}_{n+1}\big], \tag{3}$$

and the equations of motion and position kinematic constraint are discretized into

$$\frac{1}{1+\alpha}(\boldsymbol{M}\boldsymbol{a})_{n+1} + \big(\boldsymbol{\Phi}_{\boldsymbol{q}}^T\boldsymbol{\lambda} - \boldsymbol{Q}_e - \boldsymbol{Q}_s\big)_{n+1} - \frac{\alpha}{1+\alpha}\big(\boldsymbol{\Phi}_{\boldsymbol{q}}^T\boldsymbol{\lambda} - \boldsymbol{Q}_e - \boldsymbol{Q}_s\big)_n = \boldsymbol{0}, \tag{4}$$

$$\frac{1}{\beta h^2}\boldsymbol{\Phi}(\boldsymbol{q}_{n+1}, t_{n+1}) = \boldsymbol{0}, \tag{5}$$

where $\alpha$ is a selected parameter, $\beta$ and $\gamma$ are parameters depending on $\alpha$, $h$ is the time step size, $\boldsymbol{a}_{n+1}$ is an approximation of $\ddot{\boldsymbol{q}}(t_n + (1+\alpha)h)$, and the subscripts $n$ and $n+1$ mean that the related quantities should be evaluated at the $n$th and $(n+1)$-th time step, respectively.

Note that the unknowns of (4) and (5) are $\boldsymbol{a}_{n+1}$ and $\boldsymbol{\lambda}_{n+1}$. The associated Jacobian matrix is [30]

$$\boldsymbol{J} = \begin{bmatrix} \frac{1}{1+\alpha}\boldsymbol{M} + \beta h^2(\boldsymbol{M}\boldsymbol{a} + \boldsymbol{\Phi}_{\boldsymbol{q}}^T\boldsymbol{\lambda} - \boldsymbol{Q}_e - \boldsymbol{Q}_s)_{\boldsymbol{q}} - \gamma h(\boldsymbol{Q}_e)_{\dot{\boldsymbol{q}}} & \boldsymbol{\Phi}_{\boldsymbol{q}}^T \\ \boldsymbol{\Phi}_{\boldsymbol{q}} & \boldsymbol{0} \end{bmatrix}. \tag{6}$$

As shown in (6), an efficient way is needed to evaluate the derivatives of general forces with respect to state variables.

One of the advantages of this method is the good conditioning of the Jacobian matrix associated with the implicit integrator. It can be easily found that when $h \to 0$, $\boldsymbol{J}$ is nonsingular as long as $\boldsymbol{M}$ is nonsingular and the kinematic constraints are independent.

**Fig. 1** Pseudocode of the HHT-I3 algorithm

$t_{n+1} = t_n + h$

$\boldsymbol{w}_{n+1}^{(0)} = \boldsymbol{w}_n$

**while** $|\boldsymbol{\upsilon}| > \vartheta_1$ or $|\triangle \boldsymbol{w}| > \vartheta_2$ **do**

  Update $\boldsymbol{q}_{n+1}^{(k)}$ and $\dot{\boldsymbol{q}}_{n+1}^{(k)}$ using Eqn. (2) and (3)

  Evalute Jacobian $\boldsymbol{J}$

  Solve linear system $\boldsymbol{J} \triangle \boldsymbol{w}^{(k)} = \boldsymbol{\upsilon}\left(\boldsymbol{w}_{n+1}^{(k)}\right)$

  $\boldsymbol{w}_{n+1}^{(k+1)} = \boldsymbol{w}_{n+1}^{(k)} - \triangle \boldsymbol{w}^{(k)}$

**end**

$\boldsymbol{w}_{n+1} = \boldsymbol{w}_{n+1}^{(k)}$

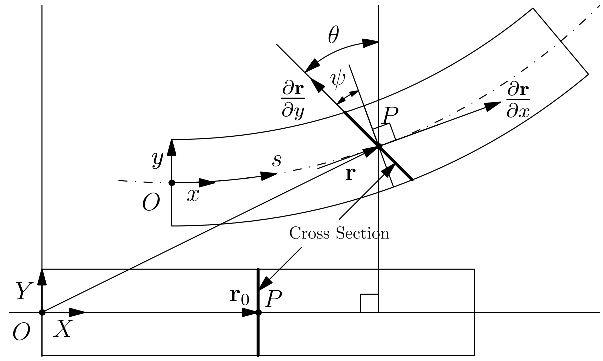


**Fig. 2** Planar shear-deformable beam element

The pseudocode of the HHT-I3 algorithm from time step $n$ to $n+1$ is shown in Fig. 1, where $\boldsymbol{w} = [\boldsymbol{a}^T \quad \boldsymbol{\lambda}^T]^T$, $\boldsymbol{\upsilon}$ is the vector of residual of (4) and (5), and $\vartheta_1$ and $\vartheta_2$ are user specified tolerances.

The accuracy and efficiency of this algorithm have been investigated in detail [22, 29, 30]. One of the most expensive tasks when HHT-I3 algorithm is employed is the calculus of the Jacobian matrix. Taking advantage of ANCF, the Jacobian matrix can be exactly and efficiently evaluated as shown in the following sections, which greatly reduces the computational cost compared with numerical differentiation techniques.

## 2.2 Kinematics of flexible multibody systems based on ANCF

In this paper, a two dimensional shear deformable beam is taken as an example to illustrate the procedures of dynamic and sensitivity analysis of ANCF-based flexible multibody systems, as shown in Fig. 2.

Vector $\boldsymbol{r}$ is the global position vector of an arbitrary point $P$ in the beam cross section, $x$ and $y$ are the coordinates of $P$ defined in the beam coordinate system. In the shear deformable beam model, the cross section of the beam does not remain normal to the neutral axis. As shown in Fig. 2, angles $\theta$ and $\psi$ account for the overall rotation of the cross section and the shear angle, respectively.

The global position vector of point $P$ can be written as

$$\boldsymbol{r} = [r_1 \quad r_2]^T = \boldsymbol{S}\boldsymbol{e}, \tag{7}$$

where $\boldsymbol{S}$ is the global element shape function, and $\boldsymbol{e}$ is the vector of nodal coordinates.

The element shape function $\boldsymbol{S}$ can be defined as

$$\boldsymbol{S}=\begin{bmatrix} s_1 & 0 & ls_2 & 0 & ls_3 & 0 & s_4 & 0 & ls_5 & 0 & ls_6 & 0 \\ 0 & s_1 & 0 & ls_2 & 0 & ls_3 & 0 & s_4 & 0 & ls_5 & 0 & ls_6 \end{bmatrix} \tag{8}$$

where

$$s_1 = 1-3\xi^2+2\xi^3, \qquad s_2=\xi-2\xi^2+\xi^3, \qquad s_3=\eta-\xi\eta,$$
$$s_4=3\xi^2-2\xi^3, \qquad s_5=-\xi^2+\xi^3, \qquad s_6=\xi\eta,$$

and $\xi = x/l$, $\eta = y/l$; $l$ is the element length.

The vector of the element nodal coordinates $\boldsymbol{e}=[e_1\ \dots\ e_{12}]^T$ is given by

$$e_1=r_1|_{x=0}, \qquad e_2=r_2|_{x=0}, \qquad e_3=\left.\frac{\partial r_1}{\partial x}\right|_{x=0}, \qquad e_4=\left.\frac{\partial r_2}{\partial x}\right|_{x=0},$$
$$e_5=\left.\frac{\partial r_1}{\partial y}\right|_{x=0}, \qquad e_6=\left.\frac{\partial r_2}{\partial y}\right|_{x=0}, \qquad e_7=r_1\,|_{x=l}, \qquad e_8=r_2\,|_{x=l},$$
$$e_9=\left.\frac{\partial r_1}{\partial x}\right|_{x=l}, \qquad e_{10}=\left.\frac{\partial r_2}{\partial x}\right|_{x=l}, \qquad e_{11}=\left.\frac{\partial r_1}{\partial y}\right|_{x=l}, \qquad e_{12}=\left.\frac{\partial r_2}{\partial y}\right|_{x=l}.$$

## 2.3 Mass matrix

One of the most attractive characteristics of ANCF is that the mass matrix $\boldsymbol{M}$ in (1) remains constant during dynamic simulation. To achieve this goal, the element mass matrix $\boldsymbol{M}_e$ is derived at first and then assembled using the standard finite element procedure.

The kinetic energy of the element is defined as

$$T=\frac{1}{2}\int_V \rho\dot{\boldsymbol{r}}^T\dot{\boldsymbol{r}}\,dV=\frac{1}{2}\dot{\boldsymbol{e}}^T\left(\int_V \rho\boldsymbol{S}^T\boldsymbol{S}\,dV\right)\dot{\boldsymbol{e}}=\frac{1}{2}\dot{\boldsymbol{e}}^T\boldsymbol{M}_e\dot{\boldsymbol{e}}, \tag{9}$$

where $V$ is the element volume, $\rho$ is the mass density of the beam material, $\dot{\boldsymbol{r}}=\boldsymbol{S}\dot{\boldsymbol{e}}$ is the absolute velocity vector and $\boldsymbol{M}_e$ is the mass matrix of the element defined as

$$\boldsymbol{M}_e=\int_V \rho\boldsymbol{S}^T\boldsymbol{S}\,dV. \tag{10}$$

It can be easily deduced that $\boldsymbol{M}_e$ is constant and symmetric.

## 2.4 Generalized forces

### *2.4.1 Generalized external forces*

Suppose that an external force $\boldsymbol{F}_e$ is applied to an arbitrary point of the beam element, the virtual work due to the force is [32]

$$\delta W_e=\boldsymbol{F}_e^T\delta\boldsymbol{r}=\boldsymbol{F}_e^T\boldsymbol{S}\delta\boldsymbol{e}=\boldsymbol{Q}_e^T\delta\boldsymbol{e}, \tag{11}$$

where $\boldsymbol{Q}_e$ is the vector of generalized external forces. Taking the gravity force, for example, the vector of generalized distributed gravity forces is

$$\boldsymbol{Q}_e = -\rho V g \begin{bmatrix} 0 & \frac{1}{2} & 0 & \frac{l}{12} & 0 & 0 & 0 & \frac{1}{2} & 0 & -\frac{l}{12} & 0 & 0 \end{bmatrix}^T. \tag{12}$$

### *2.4.2 Generalized elastic forces*

Elastic forces based on ANCF are the only nonlinear terms in (1). To efficiently evaluate the elastic forces, many investigations have been made [2, 3, 14, 27, 38]. An efficient approach is proposed in [14], in which the elastic forces vector $\boldsymbol{Q}_s$ is written as

$$\boldsymbol{Q}_s = -\big(\boldsymbol{K}_2(\boldsymbol{e},\boldsymbol{b}) + \boldsymbol{K}_1(\boldsymbol{b})\big)\boldsymbol{e} \tag{13}$$

where

$$\begin{aligned}\boldsymbol{K}_2 = {} & \frac{\kappa+2G}{2}\left(\int_V \boldsymbol{S}_{,1}^T\boldsymbol{S}_{,1}\boldsymbol{e}\boldsymbol{e}^T\boldsymbol{S}_{,1}^T\boldsymbol{S}_{,1}\,dV + \int_V \boldsymbol{S}_{,2}^T\boldsymbol{S}_{,2}\boldsymbol{e}\boldsymbol{e}^T\boldsymbol{S}_{,2}^T\boldsymbol{S}_{,2}\,dV\right)\\ & + \frac{\kappa}{2}\left(\int_V \boldsymbol{S}_{,1}^T\boldsymbol{S}_{,1}\boldsymbol{e}\boldsymbol{e}^T\boldsymbol{S}_{,2}^T\boldsymbol{S}_{,2}\,dV + \int_V \boldsymbol{S}_{,2}^T\boldsymbol{S}_{,2}\boldsymbol{e}\boldsymbol{e}^T\boldsymbol{S}_{,1}^T\boldsymbol{S}_{,1}\,dV\right)\\ & + G\left(\int_V \boldsymbol{S}_{,1}^T\boldsymbol{S}_{,2}\boldsymbol{e}\boldsymbol{e}^T\boldsymbol{S}_{,2}^T\boldsymbol{S}_{,1}\,dV + \int_V \boldsymbol{S}_{,2}^T\boldsymbol{S}_{,1}\boldsymbol{e}\boldsymbol{e}^T\boldsymbol{S}_{,1}^T\boldsymbol{S}_{,2}\,dV\right)\end{aligned} \tag{14}$$

and

$$\boldsymbol{K}_1 = -(\kappa+G)\left(\int_V \boldsymbol{S}_{,1}^T\boldsymbol{S}_{,1}\,dV + \int_V \boldsymbol{S}_{,2}^T\boldsymbol{S}_{,2}\,dV\right). \tag{15}$$

In the above equations, $\kappa$ is the Lamé's constant and $G$ is the shear modulus of the material. The $i$th row of matrix $\boldsymbol{S}_{,j}$ is defined as

$$(\boldsymbol{S}_{,j})_i = \left(\frac{\partial \boldsymbol{x}}{\partial \boldsymbol{r}_o}\right)_j^T \begin{bmatrix} \boldsymbol{S}_{i,x}^T & \boldsymbol{S}_{i,y}^T \end{bmatrix}^T, \quad i,j = 1,2, \tag{16}$$

where $(\partial\boldsymbol{x}/\partial\boldsymbol{r}_o)_j^T$ is the $j$-th row of $(\partial\boldsymbol{x}/\partial\boldsymbol{r}_o)^T$, $\boldsymbol{x} = [x \;\; y]^T$, $\boldsymbol{r}_o = \boldsymbol{S}\boldsymbol{e}_o$ represents any arbitrary material point in the reference configuration defined by $\boldsymbol{e}_o$, $\boldsymbol{S}_{i,x}$ and $\boldsymbol{S}_{i,y}$ are the derivatives of the $i$th row of the shape function with respect to $x$ and $y$, respectively.

To separate the state variables from other parameters of the elastic forces, a tensor transformation is introduced and a typical element of $\boldsymbol{K}_2$ is written as

$$\boldsymbol{K}_2^{ij} = \boldsymbol{e}^T\boldsymbol{C}_{\boldsymbol{K}_2}^{ij}\boldsymbol{e}, \tag{17}$$

where

$$\begin{aligned}\boldsymbol{C}_{\boldsymbol{K}_2}^{ij} = {} & \frac{\kappa+2G}{2}\int_V \Big(\big(\boldsymbol{S}_{,1}^T\boldsymbol{S}_{,1}\big)_i^T\big(\boldsymbol{S}_{,1}^T\boldsymbol{S}_{,1}\big)_j + \big(\boldsymbol{S}_{,2}^T\boldsymbol{S}_{,2}\big)_i^T\big(\boldsymbol{S}_{,2}^T\boldsymbol{S}_{,2}\big)_j\Big)\,dV\\ & + \frac{\kappa}{2}\int_V \Big(\big(\boldsymbol{S}_{,1}^T\boldsymbol{S}_{,1}\big)_i^T\big(\boldsymbol{S}_{,2}^T\boldsymbol{S}_{,2}\big)_j + \big(\boldsymbol{S}_{,2}^T\boldsymbol{S}_{,2}\big)_i^T\big(\boldsymbol{S}_{,1}^T\boldsymbol{S}_{,1}\big)_j\Big)\,dV\\ & + G\int_V \Big(\big(\boldsymbol{S}_{,1}^T\boldsymbol{S}_{,2}\big)_i^T\big(\boldsymbol{S}_{,2}^T\boldsymbol{S}_{,1}\big)_j + \big(\boldsymbol{S}_{,2}^T\boldsymbol{S}_{,1}\big)_i^T\big(\boldsymbol{S}_{,1}^T\boldsymbol{S}_{,2}\big)_j\Big)\,dV.\end{aligned} \tag{18}$$

As shown in (15) and (18), matrices $\boldsymbol{K}_1$ and $\boldsymbol{C}^{ij}_{\boldsymbol{K}_2}$ are independent of $\boldsymbol{e}$ and $t$, which means that matrices $\boldsymbol{K}_1$ and $\boldsymbol{C}^{ij}_{\boldsymbol{K}_2}$ are invariant and can be prepared in advance. The generalized elastic forces are able to be calculated through matrix multiplication with these invariant matrices instead of the conventional numerical integration procedure, which considerably reduces the computational expenses during simulation [14].

### 2.5 Jacobian of the elastic forces

There is a need to evaluate the derivatives of the generalized elastic forces with respect to state variables in accordance with the invoked integration method. Using invariant matrices $\boldsymbol{K}_1$ and $\boldsymbol{C}^{ij}_{\boldsymbol{K}_2}$ described above, any arbitrary component of these derivatives is written as [14]

$$\left(\frac{\partial \boldsymbol{Q}_s}{\partial \boldsymbol{e}}\right)_{ik} = \frac{\partial \boldsymbol{Q}_{si}}{\partial e_k} = -\boldsymbol{e}^T \boldsymbol{C}^{ik}_{\boldsymbol{K}_2}\boldsymbol{e} - \boldsymbol{K}_{1ik} - \sum_j \sum_m e_m \left(\boldsymbol{C}^{ij}_{\boldsymbol{K}_2} + \boldsymbol{C}^{ijT}_{\boldsymbol{K}_2}\right)_{mk} e_j. \tag{19}$$

As presented in (19), the Jacobian of generalized elastic forces can also be evaluated exactly and efficiently with matrix multiplication.

## 3 First order sensitivity analysis of ANCF-based flexible multibody systems

### 3.1 Objective function of optimization

An objective function must be specified for optimizing the performance of a multibody system. A widely used objective function investigated in this article takes on the form

$$\Psi = \int_{t_1}^{t_2} H\left(t, \boldsymbol{q}(t, \boldsymbol{b}), \dot{\boldsymbol{q}}(t, \boldsymbol{b}), \boldsymbol{\lambda}(t, \boldsymbol{b}), \boldsymbol{b}\right) dt, \tag{20}$$

where $t_1$ and $t_2$, assumed to be known, are the initial and final time of dynamic simulation, respectively. The state variables $\boldsymbol{q}$, $\dot{\boldsymbol{q}}$ and Lagrange multipliers $\boldsymbol{\lambda}$ are functions of the design variables.

To evaluate the design sensitivity, applying Leibnitz's and the chain rule of differentiation yields

$$\frac{d\Psi}{d\boldsymbol{b}} = \int_{t_1}^{t_2} \left(H_{\boldsymbol{q}}\boldsymbol{q}_{\boldsymbol{b}} + H_{\dot{\boldsymbol{q}}}\dot{\boldsymbol{q}}_{\boldsymbol{b}} + H_{\boldsymbol{\lambda}}\boldsymbol{\lambda}_{\boldsymbol{b}} + H_{\boldsymbol{b}}\right) dt \tag{21}$$

where the derivative of a scalar with respect to a column vector is defined as a row vector. To evaluate (21), the direct differentiation method and adjoint variable method are performed in this article as follows.

### 3.2 Direct differentiation method

The direct differentiation method differentiates (1) with respect to vector $\boldsymbol{b}$, which yields

$$\begin{aligned} \boldsymbol{M}\ddot{\boldsymbol{q}}_{\boldsymbol{b}} + \boldsymbol{\Phi}_{\boldsymbol{q}}^T\boldsymbol{\lambda}_{\boldsymbol{b}} = &-\left(\boldsymbol{M}\hat{\ddot{\boldsymbol{q}}}\right)_{\boldsymbol{b}} - \left(\boldsymbol{M}\hat{\ddot{\boldsymbol{q}}}\right)_{\boldsymbol{q}}\boldsymbol{q}_{\boldsymbol{b}} - \left(\boldsymbol{\Phi}_{\boldsymbol{q}}^T\hat{\boldsymbol{\lambda}}\right)_{\boldsymbol{b}} - \left(\boldsymbol{\Phi}_{\boldsymbol{q}}^T\hat{\boldsymbol{\lambda}}\right)_{\boldsymbol{q}}\boldsymbol{q}_{\boldsymbol{b}} \\ &+ (\boldsymbol{Q}_e + \boldsymbol{Q}_s)_{\boldsymbol{b}} + (\boldsymbol{Q}_e + \boldsymbol{Q}_s)_{\boldsymbol{q}}\boldsymbol{q}_{\boldsymbol{b}} + (\boldsymbol{Q}_e)_{\dot{\boldsymbol{q}}}\dot{\boldsymbol{q}}_{\boldsymbol{b}}, \end{aligned} \tag{22}$$

$$\boldsymbol{\Phi}_{\boldsymbol{q}}\boldsymbol{q}_{\boldsymbol{b}} + \boldsymbol{\Phi}_{\boldsymbol{b}} = \boldsymbol{0}, \tag{23}$$

where a hat "ˆ" over a term means that the term is held constant during differentiation. The above procedure is usually realized with symbolic differentiation method. Suppose $\boldsymbol{b}$ is a vector of dimension $n$, (22) and (23) compose $n$ DAE systems of index-3 for unknowns $\boldsymbol{q_b}$ and $\boldsymbol{\lambda_b}$. The HHT-I3 method is introduced again to integrate the sensitivity DAEs, and (21) is then evaluated to obtain the objective sensitivities.

However, according to the features of ANCF illustrated in Sect. 2, it can be found that term $(\boldsymbol{M}\hat{\ddot{\boldsymbol{q}}})_{\boldsymbol{q}}$ vanishes because mass matrix $\boldsymbol{M}$ is independent of $\boldsymbol{q}$. Besides that, all the terms in (22) can be exactly evaluated as follows:

$\boldsymbol{M}, \boldsymbol{\Phi}_{\boldsymbol{q}}^T, (\boldsymbol{Q}_e + \boldsymbol{Q}_s)_{\boldsymbol{q}}, (\boldsymbol{Q}_e)_{\dot{\boldsymbol{q}}}$: These items can be assembled and exactly evaluated with the same method as in dynamic analysis.

$(\boldsymbol{M}\hat{\ddot{\boldsymbol{q}}})_{\boldsymbol{b}}$: The procedure to deduce this item can be divided into three steps. Firstly, the derivatives of element mass matrix $\boldsymbol{M}_e$ with respect to a specific design variable $b$ are obtained analytically. Secondly, the derivatives above are assembled using finite element procedure to get $\boldsymbol{M}_b$. Finally, $(\boldsymbol{M}\hat{\ddot{\boldsymbol{q}}})_b$ is obtained by multiplying $\boldsymbol{M}_b$ by $\hat{\ddot{\boldsymbol{q}}}$, which is used as a constant vector in the process of sensitivity analysis.

$(\boldsymbol{Q}_e)_{\boldsymbol{b}}$: As shown in Sect. 2.4.1, the generalized external forces vector $\boldsymbol{Q}_e$ takes on a simple form. $(\boldsymbol{Q}_e)_{\boldsymbol{b}}$ can be easily deduced by differentiating $\boldsymbol{Q}_e$ with respect to $\boldsymbol{b}$.

$(\boldsymbol{Q}_s)_{\boldsymbol{b}}$: The generalized elastic forces vector $\boldsymbol{Q}_s$ is defined in (13). $(\boldsymbol{Q}_s)_{\boldsymbol{b}}$ is obtained by taking the derivative of (13) with respect to a specific design variable $b$ as

$$(\boldsymbol{Q}_s)_b = -\big((\boldsymbol{K}_2)_b + (\boldsymbol{K}_1)_b\big)\boldsymbol{e}. \tag{24}$$

$(\boldsymbol{K}_1)_b$ can be prepared in advance because $\boldsymbol{K}_1$ is invariant as shown in (15). Any arbitrary element of $(\boldsymbol{K}_2)_b$ is defined as

$$\big(\boldsymbol{K}_2\big)_b^{ij} = \boldsymbol{e}^T\big(\boldsymbol{C}_{\boldsymbol{K}_2}^{ij}\big)_b\boldsymbol{e} \tag{25}$$

where $(\boldsymbol{C}_{\boldsymbol{K}_2}^{ij})_b$ can also be prepared beforehand for the same reason as $(\boldsymbol{K}_1)_b$.

$(\boldsymbol{\Phi}_{\boldsymbol{q}}^T\hat{\boldsymbol{\lambda}})_{\boldsymbol{b}}, (\boldsymbol{\Phi}_{\boldsymbol{q}}^T\hat{\boldsymbol{\lambda}})_{\boldsymbol{q}}$: The evaluation of these terms has been investigated in many papers.

The above procedure can be summarized as a new method to deduce the system sensitivity equations of ANCF-based flexible multibody systems for general purpose. The most significant advantage of this method is that element sensitivity invariant matrices $(\boldsymbol{M}_e)_{\boldsymbol{b}}$, $(\boldsymbol{K}_1)_{\boldsymbol{b}}$ and $(\boldsymbol{C}_{\boldsymbol{K}_2}^{ij})_{\boldsymbol{b}}$ can be prepared in advance along with $\boldsymbol{M}_e$, $\boldsymbol{K}_1$ and $\boldsymbol{C}_{\boldsymbol{K}_2}^{ij}$, which means that system sensitivity equations can be reformulated by assembling element sensitivity equations instead of conventional symbolic differentiation approach when the system model is changed. Furthermore, this method can greatly improve the accuracy and efficiency of construction and integration of sensitivity equations, which will be verified in the numerical experiments later.

### 3.3 Adjoint variable method

Different from direct differentiation method, the adjoint variable method does not calculate the sensitivities of state variables directly. This method introduces a set of adjoint variables to get rid of numerical integration of (22) and (23). The procedure is as follows:

1. Integrating the second term in the integral of (21) by parts yields

$$\frac{d\Psi}{d\boldsymbol{b}} = H_{\dot{q}}^2\boldsymbol{q}_{\boldsymbol{b}}^2 - H_{\dot{q}}^1\boldsymbol{q}_{\boldsymbol{b}}^1 + \int_{t_1}^{t_2}\big((H_{\boldsymbol{q}} - \dot{H}_{\dot{\boldsymbol{q}}})\boldsymbol{q}_{\boldsymbol{b}} + H_{\lambda}\boldsymbol{\lambda}_{\boldsymbol{b}} + H_{\boldsymbol{b}}\big)\,dt, \tag{26}$$

where $H_{\dot{q}}^{i}\boldsymbol{q}_{\boldsymbol{b}}^{i}$, $i=1,2$, are the quantities of $H_{\dot{q}}\boldsymbol{q}_{\boldsymbol{b}}$ evaluated at $t=t_i$, $i=1,2$, respectively.

2. Multiplying (22) and (23) by the transpose of introduced adjoint variable vectors $\boldsymbol{\mu}$ and $\boldsymbol{\zeta}$, respectively, and integrating them over period $[t_1,t_2]$ yields

$$\int_{t_1}^{t_2}\boldsymbol{\mu}^T\big(\boldsymbol{M}\ddot{\boldsymbol{q}}_{\boldsymbol{b}}+\boldsymbol{\Phi}_q^T\boldsymbol{\lambda}_{\boldsymbol{b}}+\big(\boldsymbol{M}\hat{\ddot{\boldsymbol{q}}}\big)_{\boldsymbol{b}}+\big(\boldsymbol{M}\hat{\ddot{\boldsymbol{q}}}\big)_q\boldsymbol{q}_{\boldsymbol{b}}+\big(\boldsymbol{\Phi}_q^T\hat{\boldsymbol{\lambda}}\big)_{\boldsymbol{b}}+\big(\boldsymbol{\Phi}_q^T\hat{\boldsymbol{\lambda}}\big)_q\boldsymbol{q}_{\boldsymbol{b}}$$

$$-(\boldsymbol{Q}_e+\boldsymbol{Q}_s)_{\boldsymbol{b}}-(\boldsymbol{Q}_e+\boldsymbol{Q}_s)_q\boldsymbol{q}_{\boldsymbol{b}}-(\boldsymbol{Q}_e)_{\dot{q}}\dot{\boldsymbol{q}}_{\boldsymbol{b}}\big)\,dt=\boldsymbol{0}, \tag{27}$$

$$\int_{t_1}^{t_2}\boldsymbol{\zeta}^T\big(\boldsymbol{\Phi}_q\boldsymbol{q}_{\boldsymbol{b}}+\boldsymbol{\Phi}_{\boldsymbol{b}}\big)\,dt=\boldsymbol{0}. \tag{28}$$

Integrating the terms involving $\ddot{\boldsymbol{q}}_{\boldsymbol{b}}$ and $\dot{\boldsymbol{q}}_{\boldsymbol{b}}$ in (27) by parts yields

$$\big(\boldsymbol{\mu}^T\boldsymbol{M}\dot{\boldsymbol{q}}_{\boldsymbol{b}}-\big(\dot{\boldsymbol{\mu}}^T\boldsymbol{M}+\boldsymbol{\mu}^T\dot{\boldsymbol{M}}\big)\boldsymbol{q}_{\boldsymbol{b}}-\boldsymbol{\mu}^T(\boldsymbol{Q}_e)_{\dot{q}}\boldsymbol{q}_{\boldsymbol{b}}\big)\big|_{t_1}^{t_2}$$

$$+\int_{t_1}^{t_2}\big[\big(\ddot{\boldsymbol{\mu}}^T\boldsymbol{M}+\boldsymbol{\mu}^T\big(\ddot{\boldsymbol{M}}+\big(\boldsymbol{M}\hat{\ddot{\boldsymbol{q}}}\big)_q+\big(\boldsymbol{\Phi}_q^T\hat{\boldsymbol{\lambda}}\big)_q+(\dot{\boldsymbol{Q}}_e)_{\dot{q}}-(\boldsymbol{Q}_e+\boldsymbol{Q}_s)_q\big)+\dot{\boldsymbol{\mu}}^T(\boldsymbol{Q}_e)_{\dot{q}}$$

$$+2\dot{\boldsymbol{\mu}}^T\dot{\boldsymbol{M}}\big)\boldsymbol{q}_{\boldsymbol{b}}+\boldsymbol{\mu}^T\big(\boldsymbol{\Phi}_q^T\boldsymbol{\lambda}_{\boldsymbol{b}}+\big(\boldsymbol{M}\hat{\ddot{\boldsymbol{q}}}\big)_{\boldsymbol{b}}+\big(\boldsymbol{\Phi}_q^T\hat{\boldsymbol{\lambda}}\big)_{\boldsymbol{b}}-(\boldsymbol{Q}_e+\boldsymbol{Q}_s)_{\boldsymbol{b}}\big)\big]\,dt=\boldsymbol{0}. \tag{29}$$

Note that mass matrix $\boldsymbol{M}$ is independent of $\boldsymbol{q}$ and $t$, so (29) can be reduced to

$$\big(\boldsymbol{\mu}^T\boldsymbol{M}\dot{\boldsymbol{q}}_{\boldsymbol{b}}-\dot{\boldsymbol{\mu}}^T\boldsymbol{M}\boldsymbol{q}_{\boldsymbol{b}}-\boldsymbol{\mu}^T(\boldsymbol{Q}_e)_{\dot{q}}\boldsymbol{q}_{\boldsymbol{b}}\big)\big|_{t_1}^{t_2}$$

$$+\int_{t_1}^{t_2}\big[\big(\ddot{\boldsymbol{\mu}}^T\boldsymbol{M}+\boldsymbol{\mu}^T\big(\big(\boldsymbol{\Phi}_q^T\hat{\boldsymbol{\lambda}}\big)_q+(\dot{\boldsymbol{Q}}_e)_{\dot{q}}-(\boldsymbol{Q}_e+\boldsymbol{Q}_s)_q\big)+\dot{\boldsymbol{\mu}}^T(\boldsymbol{Q}_e)_{\dot{q}}\big)\boldsymbol{q}_{\boldsymbol{b}}$$

$$+\boldsymbol{\mu}^T\big(\boldsymbol{\Phi}_q^T\boldsymbol{\lambda}_{\boldsymbol{b}}+\big(\boldsymbol{M}\hat{\ddot{\boldsymbol{q}}}\big)_{\boldsymbol{b}}+\big(\boldsymbol{\Phi}_q^T\hat{\boldsymbol{\lambda}}\big)_{\boldsymbol{b}}-(\boldsymbol{Q}_e+\boldsymbol{Q}_s)_{\boldsymbol{b}}\big)\big]\,dt=\boldsymbol{0}. \tag{30}$$

Note that vector $\boldsymbol{0}$ on the right side of (27), (28), (29), and (30) is a row vector with the same dimension as that of $\boldsymbol{b}$.

3. To make the terms containing $\dot{\boldsymbol{q}}_{\boldsymbol{b}}^2$ and $\boldsymbol{q}_{\boldsymbol{b}}^2$ equal to zero in (30), taking the derivatives of velocity constraints

$$\boldsymbol{\Phi}_q(\boldsymbol{q},\boldsymbol{b})\dot{\boldsymbol{q}}=\boldsymbol{0} \tag{31}$$

with respect to $\boldsymbol{b}$ gives

$$(\boldsymbol{\Phi}_q\dot{\boldsymbol{q}})_q\boldsymbol{q}_{\boldsymbol{b}}+\big(\boldsymbol{\Phi}_q\hat{\dot{\boldsymbol{q}}}\big)_{\boldsymbol{b}}+\boldsymbol{\Phi}_q\dot{\boldsymbol{q}}_{\boldsymbol{b}}=\boldsymbol{0}. \tag{32}$$

Multiplying (23) and (32) by the transpose of introduced vectors $\boldsymbol{\gamma}$ and $\boldsymbol{\varepsilon}$, respectively, and evaluating them at the final time $t_2$ yields

$$\boldsymbol{\gamma}^{2T}\big(\boldsymbol{\Phi}_q^2\boldsymbol{q}_{\boldsymbol{b}}^2+\boldsymbol{\Phi}_{\boldsymbol{b}}^2\big)=\boldsymbol{0}, \tag{33}$$

$$\boldsymbol{\varepsilon}^{2T}\big((\boldsymbol{\Phi}_q\dot{\boldsymbol{q}})_q^2\boldsymbol{q}_{\boldsymbol{b}}^2+\big(\boldsymbol{\Phi}_q\hat{\dot{\boldsymbol{q}}}\big)_{\boldsymbol{b}}^2+\boldsymbol{\Phi}_q^2\dot{\boldsymbol{q}}_{\boldsymbol{b}}^2\big)=\boldsymbol{0}. \tag{34}$$

4. Subtracting the left side of (28), (30), (33), and (34) from (26) gives

$$\frac{d\Psi}{d\boldsymbol{b}}=\int_{t_1}^{t_2}\Big[H_q-\dot{H}_{\dot{q}}-\ddot{\boldsymbol{\mu}}^T\boldsymbol{M}-\boldsymbol{\mu}^T\big(\big(\boldsymbol{\Phi}_q^T\hat{\boldsymbol{\lambda}}\big)_q+(\dot{\boldsymbol{Q}}_e)_{\dot{q}}-(\boldsymbol{Q}_e+\boldsymbol{Q}_s)_q\big)$$

$$- \dot{\boldsymbol{\mu}}^T (\boldsymbol{Q}_e)_{\dot{q}} - \boldsymbol{\zeta}^T \boldsymbol{\Phi}_q \Big] \boldsymbol{q}_b \, dt + \int_{t_1}^{t_2} \big(H_\lambda - \boldsymbol{\mu}^T \boldsymbol{\Phi}_q^T\big) \boldsymbol{\lambda}_b \, dt$$
$$+ \int_{t_1}^{t_2} \Big(H_b - \boldsymbol{\mu}^T \big( (\boldsymbol{M} \hat{\ddot{\boldsymbol{q}}})_b + (\boldsymbol{\Phi}_q^T \hat{\boldsymbol{\lambda}})_b - (\boldsymbol{Q}_e + \boldsymbol{Q}_s)_b \big) - \boldsymbol{\zeta}^T \boldsymbol{\Phi}_b \Big) dt$$
$$+ \big( \dot{\boldsymbol{\mu}}^{2T} \boldsymbol{M} - \boldsymbol{\gamma}^{2T} \boldsymbol{\Phi}_q^2 - \boldsymbol{\varepsilon}^{2T} (\boldsymbol{\Phi}_q \dot{\boldsymbol{q}})_q^2 + \boldsymbol{\mu}^{2T} (\boldsymbol{Q}_e)_{\dot{q}}^2 + H_{\dot{q}}^2 \big) \boldsymbol{q}_b^2$$
$$- \big( \boldsymbol{\mu}^{2T} \boldsymbol{M} + \boldsymbol{\varepsilon}^{2T} \boldsymbol{\Phi}_q^2 \big) \dot{\boldsymbol{q}}_b^2 + \boldsymbol{\mu}^{1T} \boldsymbol{M} \dot{\boldsymbol{q}}_b^1$$
$$- \big( H_{\dot{q}}^1 + \dot{\boldsymbol{\mu}}^{1T} \boldsymbol{M} + \boldsymbol{\mu}^{1T} (\boldsymbol{Q}_e)_{\dot{q}}^1 \big) \boldsymbol{q}_b^1 - \boldsymbol{\gamma}^{2T} \boldsymbol{\Phi}_b^2 - \boldsymbol{\varepsilon}^{2T} (\boldsymbol{\Phi}_q \hat{\dot{\boldsymbol{q}}})_b^2. \tag{35}$$

Selecting the adjoint variables such that the coefficients of $\boldsymbol{q}_b$, $\boldsymbol{\lambda}_b$, $\boldsymbol{q}_b^2$, and $\dot{\boldsymbol{q}}_b^2$ are equal to zero yields the following set of adjoint equations:

$$\boldsymbol{M} \ddot{\boldsymbol{\mu}} + \boldsymbol{\Phi}_q^T \boldsymbol{\zeta} = H_q^T - \dot{H}_{\dot{q}}^T - (\boldsymbol{Q}_e)_{\dot{q}}^T \dot{\boldsymbol{\mu}} - \Big[ (\boldsymbol{\Phi}_q^T \hat{\boldsymbol{\lambda}})_q^T + (\dot{\boldsymbol{Q}}_e)_{\dot{q}}^T - (\boldsymbol{Q}_e + \boldsymbol{Q}_s)_q^T \Big] \boldsymbol{\mu}, \tag{36}$$

$$\boldsymbol{\Phi}_q \boldsymbol{\mu} - H_\lambda^T = \boldsymbol{0}, \tag{37}$$

$$\boldsymbol{M} \dot{\boldsymbol{\mu}}^2 - \boldsymbol{\Phi}_q^{2T} \boldsymbol{\gamma}^2 = (\boldsymbol{\Phi}_q \dot{\boldsymbol{q}})_q^{2T} \boldsymbol{\varepsilon}^2 - (\boldsymbol{Q}_e)_{\dot{q}}^{2T} \boldsymbol{\mu}^2 - H_{\dot{q}}^{2T}, \tag{38}$$

$$\boldsymbol{M} \boldsymbol{\mu}^2 + \boldsymbol{\Phi}_q^{2T} \boldsymbol{\varepsilon}^2 = \boldsymbol{0}. \tag{39}$$

5. Equations (37) and (39) form a linear system of unknowns $\boldsymbol{\mu}^2$ and $\boldsymbol{\varepsilon}^2$ as follows:

$$\begin{bmatrix} \boldsymbol{M} & \boldsymbol{\Phi}_q^{2T} \\ \boldsymbol{\Phi}_q^2 & \boldsymbol{0} \end{bmatrix} \begin{bmatrix} \boldsymbol{\mu}^2 \\ \boldsymbol{\varepsilon}^2 \end{bmatrix} = \begin{bmatrix} \boldsymbol{0} \\ H_\lambda^{2T} \end{bmatrix}. \tag{40}$$

   $\boldsymbol{\mu}^2$ and $\boldsymbol{\varepsilon}^2$ can be obtained by solving the above linear equations.
6. The linear system of unknowns $\dot{\boldsymbol{\mu}}^2$ and $\boldsymbol{\gamma}^2$ is then constructed using (38) and the equation derived from differentiating (37) with respect to $t$ for $t = t_2$ is as follows:

$$\begin{bmatrix} \boldsymbol{M} & -\boldsymbol{\Phi}_q^{2T} \\ \boldsymbol{\Phi}_q^2 & \boldsymbol{0} \end{bmatrix} \begin{bmatrix} \dot{\boldsymbol{\mu}}^2 \\ \boldsymbol{\gamma}^2 \end{bmatrix} = \begin{bmatrix} (\boldsymbol{\Phi}_q \dot{\boldsymbol{q}})_q^{2T} \boldsymbol{\varepsilon}^2 - (\boldsymbol{Q}_e)_{\dot{q}}^{2T} \boldsymbol{\mu}^2 - H_{\dot{q}}^{2T} \\ \dot{H}_\lambda^{2T} \end{bmatrix}. \tag{41}$$

   Since $\boldsymbol{\mu}^2$ and $\boldsymbol{\varepsilon}^2$ have been obtained in the last step, $\dot{\boldsymbol{\mu}}^2$ and $\boldsymbol{\gamma}^2$ can be similarly got by calculating this linear system.
7. Backward integrating the DAE system composed of (36) and (37) using the HHT-I3 method with the initial condition $\boldsymbol{\mu}^2$ and $\dot{\boldsymbol{\mu}}^2$ derived from the last two steps yields the adjoint variables $\boldsymbol{\mu}$ and $\boldsymbol{\zeta}$ during period $[t_1, t_2]$.
8. Calculating the remaining terms in (35)

$$\frac{d\Psi}{d\boldsymbol{b}} = \int_{t_1}^{t_2} \Big(H_b - \boldsymbol{\mu}^T \big( (\boldsymbol{M} \hat{\ddot{\boldsymbol{q}}})_b + (\boldsymbol{\Phi}_q^T \hat{\boldsymbol{\lambda}})_b - (\boldsymbol{Q}_e + \boldsymbol{Q}_s)_b \big) - \boldsymbol{\zeta}^T \boldsymbol{\Phi}_b \Big) dt$$
$$+ \boldsymbol{\mu}^{1T} \boldsymbol{M} \dot{\boldsymbol{q}}_b^1 - \big( H_{\dot{q}}^1 + \dot{\boldsymbol{\mu}}^{1T} \boldsymbol{M} + \boldsymbol{\mu}^{1T} (\boldsymbol{Q}_e)_{\dot{q}}^1 \big) \boldsymbol{q}_b^1 - \boldsymbol{\gamma}^{2T} \boldsymbol{\Phi}_b^2 - \boldsymbol{\varepsilon}^{2T} (\boldsymbol{\Phi}_q \hat{\dot{\boldsymbol{q}}})_b^2 \tag{42}$$

   with $\boldsymbol{\mu}$, $\boldsymbol{\zeta}$, $\dot{\boldsymbol{\mu}}$, $\boldsymbol{\gamma}^2$, and $\boldsymbol{\varepsilon}^2$ obtained in the last steps to obtain the desired sensitivities.

As shown in (42), the adjoint variable method avoids the expensive numerical evaluation of the derivatives of state variables and Lagrange multipliers with respect to design variables.

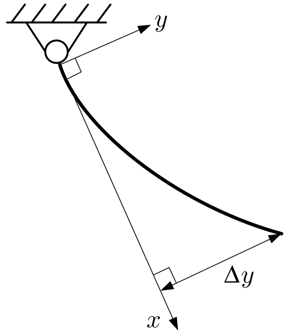


**Fig. 3** Planar single pendulum

## 4 Numerical experiments

### 4.1 Single pendulum

In this section, a planar flexible single pendulum example, as shown in Fig. 3, is presented to demonstrate the use of the proposed method in sensitivity analysis. A body coordinate frame is fixed at the left end of the beam with the $x$ axis tangent to the curve of the beam's central line. $\Delta y$ is defined as the deflection of the right end with respect to the body frame. The density, Young's modulus and Poisson ratio of the material are assumed to be 4000 kg/m$^3$, $10^7$ N/m$^2$ and 0.3, respectively. The length of the beam is chosen to be $L = 1.2$ m, the rectangular cross section is given by $h = b = 0.05$ m. The pendulum is divided into 5 elements and released from its straight and horizontal initial configurations. A 4$s$ simulation is performed with a step size of $2^{-7}$ s.

In order to see the effect of Young's modulus on the elastic deformation, the Young's modulus of the pendulum is changed to $5.0 \times 10^6$ N/m$^2$ for another simulation. The deflections and their sensitivities with respect to Young's modulus of these two pendulums are compared in Fig. 4. As expected, the first pendulum's deflections are smaller and more insensitive to the change of Young's modulus than those of the second one.

To verify the results obtained above, the sensitivity analysis of the first pendulum is performed with the finite difference method. $h$, $\rho$, and $E$ are selected as the design variables and a 1% variation in the design variables is chosen. From Fig. 5, it can be found that the direct differentiation sensitivities are comparable with the finite difference sensitivities.

This planar single pendulum can be easily extended into the spatial case. To make a comparison between the 2d and 3d cases, the spatial fully parameterized ANCF beam element proposed in [40] is employed. Sensitivities with respect to $h$, $\rho$, and $E$ in these two cases obtained by the direct differentiation method are plotted in Fig. 6. It can be found that spatial sensitivity curves coincide well with the planar curves.

### 4.2 Spatial crank-slider mechanism

In this section, a spatial crank-slider mechanism is employed as shown in Fig. 7 to make a comparison between the direct differentiation method, adjoint variable method, and finite difference method (1% variation). Both the crank and connecting rod are flexible beams and modeled using a 3-dimensional fully parameterized ANCF beam element and their detailed characteristic parameters are listed in Table 1. The slider is assumed to be massless for simplicity. The crank and connecting rod are set horizontal initially as shown in Fig. 7 and only suffer the load from gravity.

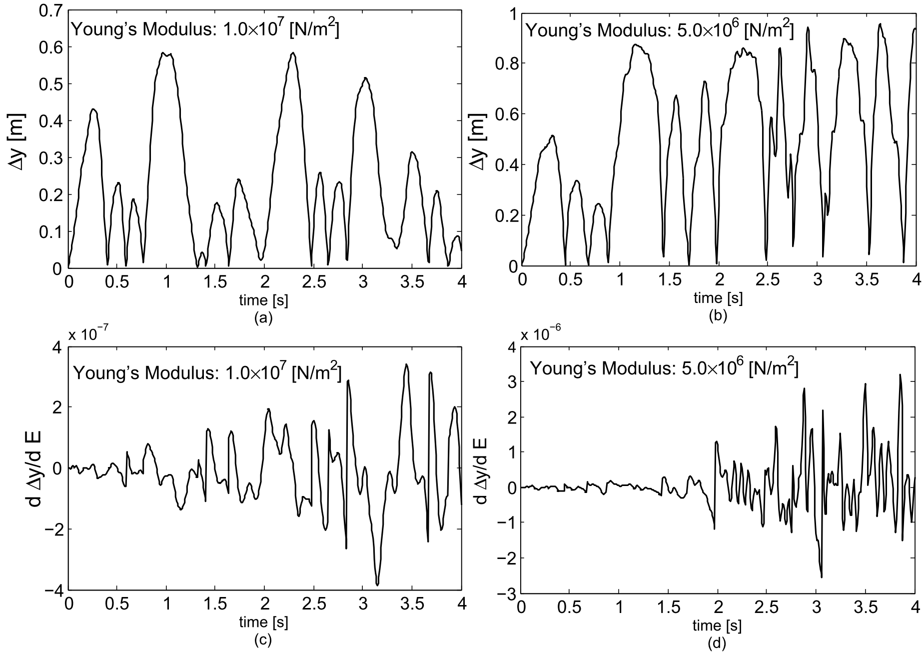


**Fig. 4** Effect of Young's modulus on elastic deformation

**Table 1** Characteristic parameters of the crank and connecting rod

| | Crank | Connecting Rod |
|---|---|---|
| Length (m) | 0.9 | 1.8 |
| Cross section ($m^2$) | $0.05 \times 0.05$ | $0.05 \times 0.05$ |
| Density ($kg/m^3$) | 2770 | 2770 |
| Young's modulus ($N/m^2$) | $1.0 \times 10^9$ | $1.0 \times 10^8$ |
| Poisson ratio | 0.3 | 0.3 |
| Number of elements | 2 | 4 |

The objective function in this example is selected as

$$\Psi = \int_0^2 (x - 1.8)^2 \, dt, \tag{43}$$

where $x$ is the slider's position coordinate in the sliding direction. The vector of design variables is selected as $\boldsymbol{b} = [h_1 \ \rho_1 \ E_1 \ h_2 \ \rho_2 \ E_2]^T$, where $h_i$, $\rho_i$, and $E_i$ are the height of cross section, density, and Young's modulus of the crank and connecting rod, respectively. Figure 8 shows the sensitivities of the slider's $x$ position coordinate using both the direct differentiation method and the finite difference method. Different from the single pendulum example, not all the sensitivity curves coincide very well. There is a big difference in the sensitivities with respect to $E_1$ and $h_2$ between these two methods. Figure 9 shows the time dependent design sensitivities of the object function obtained with all of these three methods. The results obtained with the direct differentiation method and adjoint variable

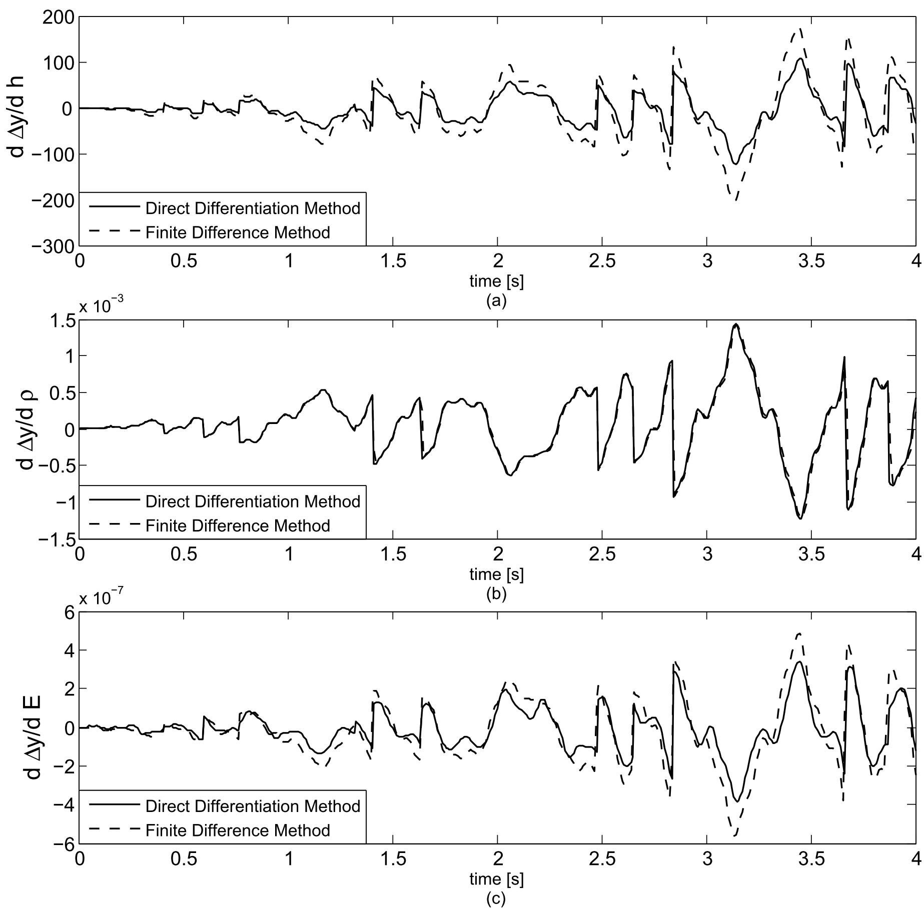


**Fig. 5** Comparison between direct differentiation method and finite difference method

method show good agreement, which demonstrates the reliability of these two methods. However, when comparing these two methods with the finite difference method, not all the obtained sensitivities coincide very well, especially with respect to the design variables $h_2$ and $E_1$, whereas in the previous single pendulum example, the finite difference method with the same variation performs much better. It can be concluded that it is not easy to select appropriate perturbations for all the design variables in all situations, which reflects the difficulties of the finite difference method mentioned in the Introduction.

The sensitivity analysis is performed on a notebook computer with an Intel Core Duo 2.53 GHz processor and 2 GB RAM in MATLAB environment. The CPU time taken in this 6 design variables example using the finite difference method, direct differentiation method, and adjoint variable method are 2922.2, 700.3, and 794.5 seconds, respectively. It is shown that the direct differentiation method is more efficient than the adjoint variable method and finite difference method. However, in some papers such as [11, 12], which adopt FFRF, the adjoint variable method is more efficient than the direct differentiation method when the number of design variables is large. In [12], the computational expense of the direct differentiation method is twice as much as that of the adjoint variable method when

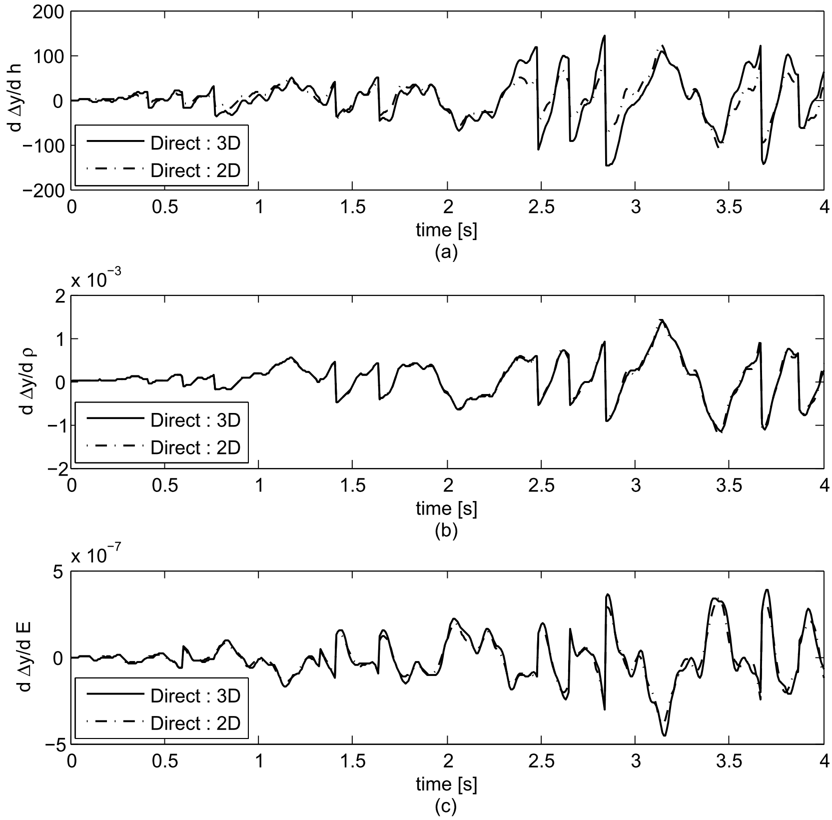


**Fig. 6** Comparison between 2D and 3D ANCF beams

**Fig. 7** Spatial slider-crank mechanism

a planar crank-slider mechanism with 5 design variables is used. The difference between the results of [12] and this article is due to the different formulations of the motion and sensitivity equations employed. When ANCF is applied, as shown in this paper, the time that the direct differentiation method needs in integrating the dynamic and sensitivity equations is less than that the forward and backward integration needs in the adjoint variable method. Thus, it can be concluded that when ANCF is utilized and the number of design variables is

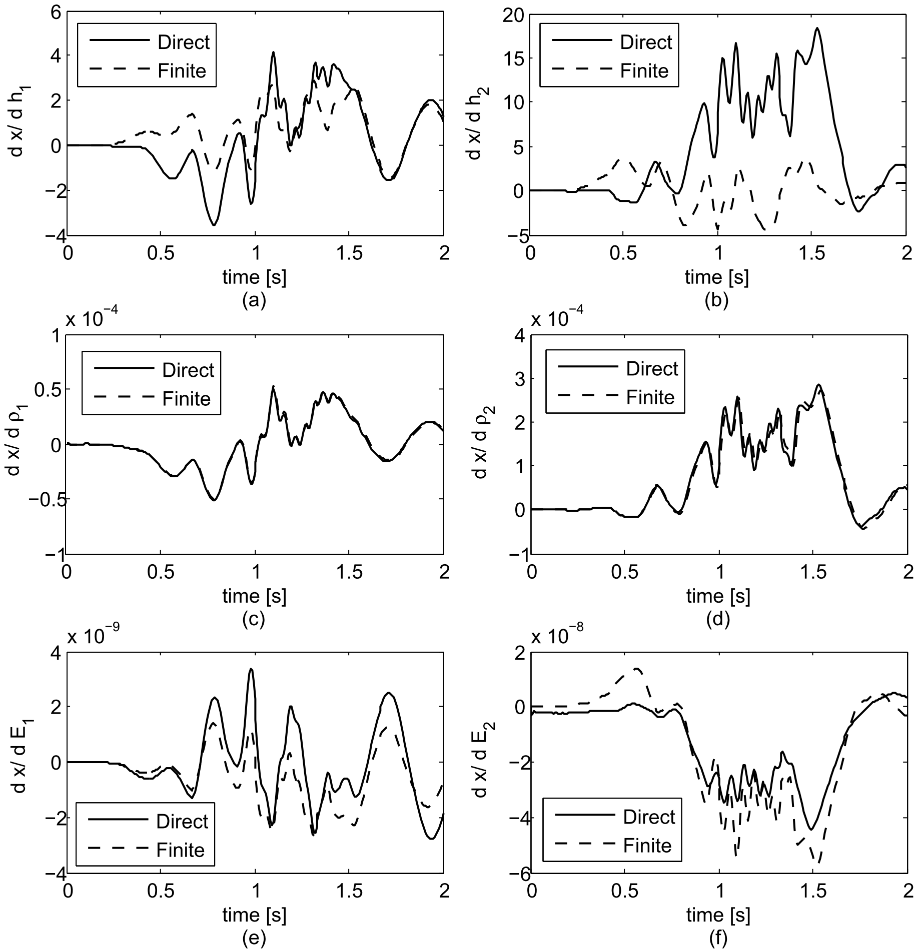


**Fig. 8** Sensitivities of the slider's *x* position coordinate w.r.t. design variables using both the finite difference method and the direct differentiation method

not extremely large, the efficiency of direct differentiation method is comparable to that of adjoint variable method.

## 5 Conclusion

In this article, ANCF is extended into the sensitivity analysis of flexible multibody systems. Both the direct differentiation method and the adjoint variable method are performed, whose feasibility and accuracy are validated through a single pendulum example and a spatial crank-slider example.

As a benefit from ANCF, a new approach to deduce the system sensitivity equations is proposed. With this approach, the system sensitivity equations are constructed by assembling the element sensitivity equations with the help of invariant matrices, which results in

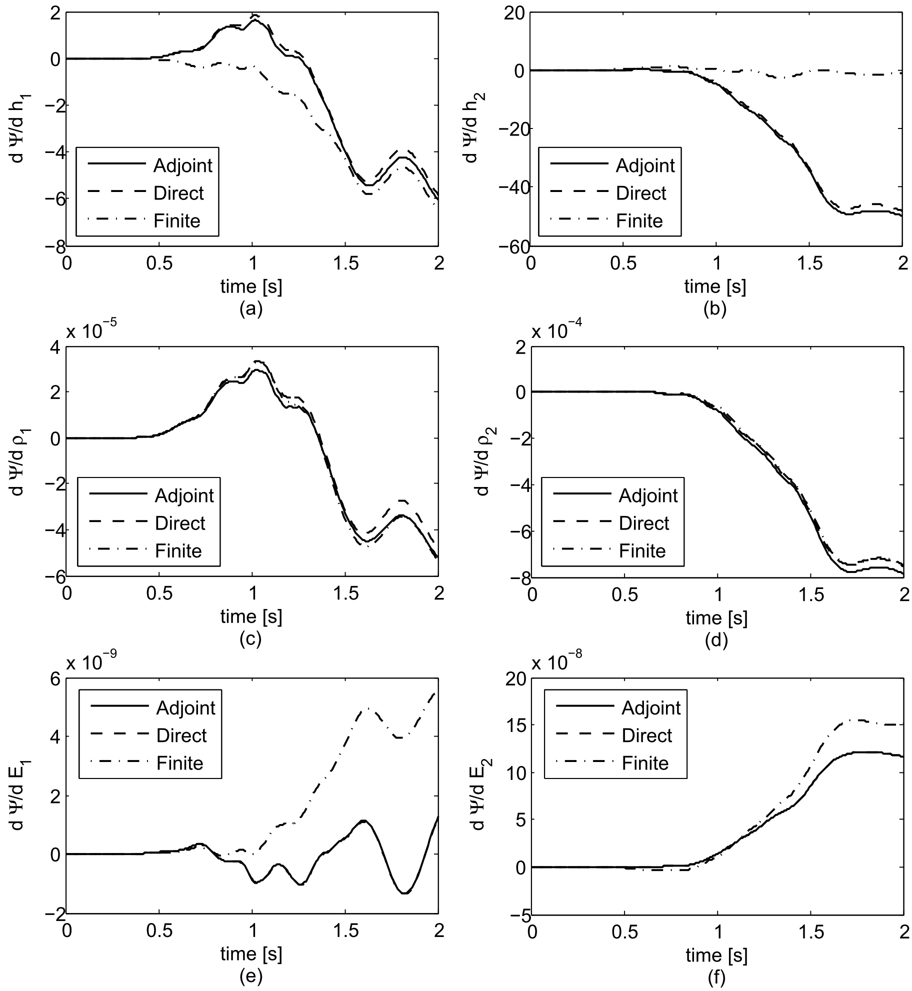


**Fig. 9** Comparison between direct differentiation method, adjoint variable method, and finite difference method

the advantage that the complex symbolic differentiation of the dynamic equations is avoided when the flexible multibody system model is changed.

Furthermore, the dynamic and sensitivity equations formed with the proposed method can be efficiently integrated using the HHT-I3 method, which makes the efficiency of the direct differentiation method comparable to that of the adjoint variable method when the number of design variables is not extremely large. All these improvements greatly enhance the application value of the direct differentiation method in the engineering optimization of the ANCF-based flexible multibody systems.

**Acknowledgements** The authors gratefully acknowledge the financial support by National High-Tech R&D Program of China (2009AA044501) and the National Natural Science Foundation of China (60704019).

## References


1. Bauchau, O.A., Laulusa, A.: Review of contemporary approaches for constraint enforcement in multibody systems. J. Comput. Nonlinear Dyn. **3**(1), 011005 (2008)
2. Berzeri, M., Shabana, A.A.: Development of simple models for the elastic forces in the absolute nodal co-ordinate formulation. J. Sound Vib. **235**(4), 539–565 (2000)
3. Berzeri, M., Campanelli, M., Shabana, A.A.: Definition of the elastic forces in the finite-element absolute nodal coordinate formulation and the floating frame of reference formulation. Multibody Syst. Dyn. **5**(1), 21–54 (2001)
4. Bestle, D., Eberhard, P.: Analyzing and optimizing multibody systems. Mech. Struct. Mach. **20**(1), 67–92 (1992)
5. Bestle, D., Seybold, J.: Sensitivity analysis of constrained multibody systems. Arch. Appl. Mech. **62**(3), 181–190 (1992)
6. Bhalerao, K., Poursina, M., Anderson, K.: An efficient direct differentiation approach for sensitivity analysis of flexible multibody systems. Multibody Syst. Dyn. **23**(2), 121–140 (2010)
7. Bischof, C., Carle, A., Corliss, G., Griewank, A., Hovland, P.: Adifor generating derivative codes from fortran programs. Sci. Program. **1**(1), 11–29 (1992)
8. Bischof, C., Khademi, P., Mauer, A., Carle, A.: Adifor 2.0: automatic differentiation of Fortran 77 programs. IEEE Comput. Sci. Eng. **3**(3), 18–32 (1996)
9. Cao, Y., Li, S., Petzold, L.: Adjoint sensitivity analysis for differential-algebraic equations: algorithms and software. J. Comput. Appl. Math. **149**(1), 171–191 (2002)
10. Chang, C.O., Nikravesh, P.E.: Optimal design of mechanical systems with constraint violation stabilization method. J. Mech. Transm. Autom. Des. **107**(4), 493–498 (1985)
11. Dias, J.M.P., Pereira, M.S.: Sensitivity analysis of Rigid-Flexible multibody systems. Multibody Syst. Dyn. **1**(3), 303–322 (1997)
12. Ding, J.Y., Pan, Z.K., Chen, L.Q.: Second order adjoint sensitivity analysis of multibody systems described by differential algebraic equations. Multibody Syst. Dyn. **18**(4), 599–617 (2007)
13. Eberhard, P.: Analysis and optimization of complex multibody systems using advanced sensitivity analysis methods. In: 3rd International Congress on Industrial and Applied Mathematics (ICIAM 95), vol. 76, pp. 40–43. Akademie Verlag, Hamburg (1995)
14. García-Vallejo, D., Mayo, J., Escalona, J.L., Domínguez, J.: Efficient evaluation of the elastic forces and the Jacobian in the absolute nodal coordinate formulation. Nonlinear Dyn. **35**(4), 313–329 (2004)
15. Greene, W.H., Haftka, R.T.: Computational aspects of sensitivity calculations in transient structural analysis. Comput. Struct. **32**(2), 433–443 (1989)
16. Griewank, A., Reese, S.: On the calculation of Jacobian matrices by the Markowitz rule. In: Griewank, A., Corliss, G. (eds.) Automatic Differentiation of Algorithms: Theory, Implementation, and Applications, pp. 126–135. SIAM, Philadelphia (1991)
17. Haftka, R.T., Gürdal, Z.: Elements of Structural Optimization, 3rd edn. Springer, Berlin (1992)
18. Haug, E.J., Ehle, P.E.: Second-order design sensitivity analysis of mechanical system dynamics. Int. J. Numer. Methods Eng. **18**(11), 1699–1717 (1982)
19. Haug, E.J., Wehage, R., Barman, N.C.: Design sensitivity analysis of planar mechanism and machine dynamics. J. Mech. Des. **103**(3), 560–570 (1981)
20. Haug, E.J., Mani, N.K., Krishnaswami, P.: Design sensitivity analysis and optimization of dynamically driven systems. In: Haug, E.J. (ed.) Computer Aided Analysis and Optimization of Mechanical System Dynamics, pp. 555–636. Springer, Heidelberg (1984)
21. Hsu, Y., Anderson, K.S.: Recursive sensitivity analysis for constrained multi-rigid-body dynamic systems design optimization. Struct. Multidiscip. Optim. **24**(4), 312–324 (2002)
22. Hussein, B., Negrut, D., Shabana, A.A.: Implicit and explicit integration in the solution of the absolute nodal coordinate differential/algebraic equations. Nonlinear Dyn. **54**(4), 283–296 (2008)
23. Laulusa, A., Bauchau, O.A.: Review of classical approaches for constraint enforcement in multibody systems. J. Comput. Nonlinear Dyn. **3**(1), 011004 (2008)
24. Li, S., Petzold, L., Zhu, W.: Sensitivity analysis of differential-algebraic equations: A comparison of methods on a special problem. Appl. Numer. Math. **32**(2), 161–174 (2000)
25. Liu, X.: Sensitivity analysis of constrained flexible multibody systems with stability considerations. Mech. Mach. Theory **31**(7), 859–863 (1996)
26. Maly, T., Petzold, L.R.: Numerical methods and software for sensitivity analysis of differential-algebraic systems. Appl. Numer. Math. **20**(1–2), 57–79 (1996)
27. Mikkola, A.M., Matikainen, M.K.: Development of elastic forces for a large deformation plate element based on the absolute nodal coordinate formulation. J. Comput. Nonlinear Dyn. **1**(2), 103–108 (2006)
28. Mukherjee, R., Bhalerao, K., Anderson, K.: A divide-and-conquer direct differentiation approach for multibody system sensitivity analysis. Struct. Multidiscip. Optim. **35**(5), 413–429 (2008)

29. Negrut, D., Rampalli, R., Ottarsson, G., Sajdak, A.: On an implementation of the Hilber–Hughes–Taylor method in the context of index 3 differential-algebraic equations of multibody dynamics (detc2005-85096). J. Comput. Nonlinear Dyn. **2**(1), 73–85 (2007)
30. Negrut, D., Jay, L.O., Khude, N.: A discussion of low-order numerical integration formulas for rigid and flexible multibody dynamics. J. Comput. Nonlinear Dyn. **4**(2), 021008 (2009)
31. Neto, M.A., Ambrózio, J.A.C., Leal, R.P.: Sensitivity analysis of flexible multibody systems using composite materials components. Int. J. Numer. Methods Eng. **77**, 386–413 (2009)
32. Omar, M.A., Shabana, A.A.: A two-dimensional shear deformable beam for large rotation and deformation problems. J. Sound Vib. **243**(3), 565–576 (2001)
33. Serban, R., Freeman, J.S.: Identification and identifiability of unknown parameters in multibody dynamic systems. Multibody Syst. Dyn. **5**(4), 335–350 (2001)
34. Serban, R., Haug, E.J.: Kinematic and kinetic derivatives in multibody system analysis. Mech. Struct. Mach. **26**(2), 145–173 (1998)
35. Shabana, A.A.: Definition of the slopes and the finite element absolute nodal coordinate formulation. Multibody Syst. Dyn. **1**(3), 339–348 (1997)
36. Shabana, A.A.: Flexible multibody dynamics: Review of past and recent developments. Multibody Syst. Dyn. **1**(2), 189–222 (1997)
37. Shabana, A.A.: Computer implementation of the absolute nodal coordinate formulation for flexible multibody dynamics. Nonlinear Dyn. **16**(3), 293–306 (1998)
38. Sopanen, J.T., Mikkola, A.M.: Description of elastic forces in absolute nodal coordinate formulation. Nonlinear Dyn. **34**(1–2), 53–74 (2003)
39. Wang, X., Haug, E.J., Pan, W.: Implicit numerical integration for design sensitivity analysis of rigid multibody systems. Mech. Based Des. Struct. Mach. **33**(1), 1–30 (2005)
40. Yakoub, R.Y., Shabana, A.A.: Three dimensional absolute nodal coordinate formulation for beam elements: Implementation and applications. J. Mech. Des. **123**(4), 614–621 (2001)